3. Mimicking Biological Carbon Isotope Signatures in Fe-C-O-H Systems

1. Introduction

The assumption of chemical equilibrium bounds much of our present theoretical understanding of natural processes. One area of research where the imposition of this assumption has particularly profound consequences, and towards which attention is drawn here, is that of carbon isotope systematics in ancient- and extraterrestrial- biosignature studies.

Of the stable isotope systems, fractionations of carbon are amongst the best understood. Despite this, the ability to differentiate between carbon of non-biological and biological origin is far from secure, as amply evidenced by ongoing controversies such as the ambiguous biogenicity of 3.8 Ga graphite in Isua, southwest Greenland (e.g. Mojzsis et al., 1996; Mojzsis and Harrison, 2000; Rosing, 1999; Schidlowski, 1988; Schidlowski, 1993; Schidlowski, 2001; van Zuilen et al., 2002; van Zuilen et al., 2003), the purported Fischer-Tropsch-type synthesis of 3.5 Ga kerogen in the Pilbara, northwest Australia (e.g. Brasier et al., 2002; Brasier et al., 2005; Schopf et al., 2002; Schopf and Packer, 1987; Ueno et al., 2004), and the origin of carbonaceous phases in meteorites (e.g. McKay et al., 1996; McSween, 1997; McSween and Harvey, 1998). Progress towards resolving these important problems affects our understanding of how, when, where and why life began.

At and above greenschist facies metamorphic conditions, carbonaceous material becomes increasingly graphitic in nature. Kerogen, loosely defined as ‘insoluble non-crystalline organic material’, is a common constituent of low-grade sedimentary rocks spanning the rock-record as far back as 3.5 Ga. Although disagreement exists in the application of the term ‘graphitic kerogen’ (e.g. Marshall et al., 2007), kerogen exhibits similar petrological behaviour (colour, reflectivity, etc.) to graphite. At temperatures considered in this study (T > 400 °C), kerogen transforms to graphite. Kerogen is therefore assumed to share the same isotopic and thermodynamic properties as

graphite. To avoid confusion, the term 'reduced carbon' is used to denote both kerogen and graphite.

This paper sets out to examine the limits on the derived isotopic signature of reduced carbon that can possibly result through both closed- and open- system equilibrium processes under geologically relevant conditions of P, T and fO_2. Calculations are performed within the thermodynamic space $1000 > P > 10000$ bar, $400 < T < 1200$ °C and $\log(fO_2^{QFM})-6 < \log(fO_2) < \log(fO_2^{QFM}) + 8$.

Because the simple molecules H_2O, O_2, H_2, CO, CO_2 and CH_4 represent the most abundant and geochemically reactive components of geological fluids (Horita, 2001), fluid thermodynamic behaviour can appropriately be described within the C-O-H system. Relevant geological processes are those that impart an isotopic fractionation on the order of that mediated by enzymatic metabolism, here considered as $\Delta\delta^{13}C \leq -15‰$ (Figure 1). Processes explicitly considered are isotopic re-equilibration with carbon in metasomatic C-O-H fluids and/or carbonate, precipitation of remobilized carbon, devolatilization of organic matter, and *de novo* carbon production resulting from decarbonation reactions of carbonates.

Under the assumption of equilibrium, the isotopic behaviour and evolution of carbon under the sway of these processes is largely quantifiable. To this end, a Modified Redlich-Kwong (MRK) equation of state built on recent thermodynamic fluid species data is coupled with recent advances in our understanding of equilibrium isotope fractionation to arrive at a versatile model for the isotopic behavior and evolution of reduced carbon interacting with C-O-H fluids in the system Fe-C-O-H. The component Fe is added to extend consideration to isotopic interaction with carbonate minerals. Because the potential for isotopic fractionation is limited at the higher decarbonation temperatures required for carbonates outside the Fe-C-O-H system (calcite, dolomite, ankerite, magnesite, rhodochrosite, etc.), restricting treatment to siderite alone is justified.

This approach uncovers the conditions under which geological equilibrium processes are capable of mimicking biological $\delta^{13}C$ fractionation. Based on these

results, the validity of the equilibrium assumption, with particular reference to Origin of Life studies, is discussed.

2. Model

2.1. The Modified Redlich-Kwong Equation of State

The modeling of fluids consisting of sub- or super- critical fluid mixtures of multiple components requires an understanding of how their chemical potentials respond to changes in state variables such as δP, δT and changes in composition, δx_i. Equations of state are equations that attempt to capture the relationship between these state variables, and thereby allow for the calculation of chemical potentials. The Redlich-Kwong equation of state (Redlich and Kwong, 1949), which incorporates parameters relevant to molecular dynamics of C-O-H fluids of interest here, takes the form:

$$P = \frac{RT}{V-b} - \frac{a}{(V^2+bV)(T)^{0.5}} \qquad (1)$$

Here, constant b accounts for repulsive forces by parameterizing molecular size and constant a accounts for intermolecular attraction. For fluids bearing molecules exhibiting a large dipole moment, such as H_2O and CO_2, a modified Redlich-Kwong ('MRK') equation was proposed (de Santis et al., 1974; Flowers, 1979; Holloway, 1984). The mixing parameters and thermodynamic constants used (after a compilation in Frost and Wood, 1995), are tabulated in Table 1 below. The MRK equation offers excellent correlation with experimental data, except at extreme metamorphic grades (P > 15000 bars, T > 1100 °C) not germane to the crustal environment (Belonoshko and Saxena, 1991; Frost and Wood, 1995; Kerrick and Jacobs, 1981).

Using this MRK equation of state, an expression for the fugacity co-efficient, ϕ_i, can be derived (Prausnitz, 1969):

$$\ln\phi_i = \ln\left(\frac{V}{V-b}\right) +$$

$$\frac{b_i}{V-b} - \frac{2\sum_{j=1}^{\hat{i}} a_{i,j}X_j}{bRT^{\frac{3}{2}}}\ln\left(\frac{V+b}{V}\right) + \frac{ab_i}{b^2RT^{\frac{3}{2}}}\left(\ln\left(\frac{V+b}{V}\right)\right) - \frac{b}{V+b}) - \ln\left(\frac{PV}{RT}\right) \qquad (2)$$

Here, $a = \sum_i \sum_j x_i x_j a_{i,j}$ and $b = \sum_i x_i b_i$. Values adopted are tabulated in Table 2.

2.2. The Reduced Carbon Saturation Surface

Phase-equilibrium experiments and other thermodynamic studies involving graphite have proven to be difficult to interpret, and have led to somewhat conflicting results. These problems stem largely from variability in the crystalline nature, ordering and thermodynamic properties of graphite (Koziol, 2004). Within the C-O-H system, the presence of reduced carbon is assumed to imply fluid saturation, with the activity of reduced carbon fixed at unity. On this reduced carbon saturation surface, pairs of C-O-H species' fugacities can now be related to one another through *P*- and *T*- dependent equilibrium constants, $k_{(i,,j)}$. In the case of reduced carbon equilibrating with the fluid components CO and CO_2, for instance:

$C + 0.5\ O_2 = CO$: $k(O_2,CO) = fCO/(fO_2)^{0.5}$

$$= \frac{\gamma CO \cdot pCO}{(\gamma O_2 \cdot pO_2)^{0.5}} = \frac{\gamma CO \cdot xCO \cdot P}{(\gamma O_2 \cdot xO_2 \cdot P)^{0.5}} \qquad (3a)$$

$C + O_2 = CO_2$: $k(O_2,CO_2) = fCO_2/fO_2$

$$= \frac{\gamma CO_2 \cdot pCO_2}{\gamma O_2 \cdot pO_2} = \frac{\gamma CO_2 \cdot xCO_2 \cdot P}{\gamma O_2 \cdot xO_2 \cdot P} \qquad (3b)$$

Similar expressions can be constructed for the other C-O-H species. The assumption of fluid ideality ($\gamma_i = x_i$), together with the condition $\sum x_i = 1$, now allows for the capture of x_i from the roots of quadratic equations (e.g. Ohmoto and Kerrick, 1977) or thermodynamic data tables (e.g. Chase, 1998). This approximate fluid composition is

used to seed an iterative re-calculation of the fugacity coefficients (Eqn. 2) and equilibria (such as Eqn. 3a,b), which converges upon the final, non-ideal fluid composition (e.g. Hall and Bodnar, 1990). The stability field of reduced carbon, together with the composition of the equilibrating fluid, is hereby laid bare in $P - T$ space by fixing any single compositional variable x_j.

2.3. Oxygen Fugacity and Reduced Carbon Stability

In addition to pressure and temperature, the geological environment often lends further constraints on the composition of C-O-H fluids by virtue of the mineral assemblage with which the fluid equilibrates. To this end, the oxygen fugacity, fO_2, provides a useful proxy. Oxygen fugacities in geological systems typically lie within +6 log units and -8 log units of the FMQ buffer, which inhabits a median position (Figure 2) amongst the commonly used buffers in $fO_2 - T$ space (Frost, 1991). The range $[\log(fO_2^{QFM}) - 6] < \log(fO_2) < [\log(fO_2^{QFM}) + 8]$ spans the buffering capabilities of a broad range of geological environments, and is adopted in this study.

Fluids outside the compositional stability field of reduced carbon (Figure 2) are prohibitively oxidizing or reducing. Here, reduced carbon is unstable with respect to CO/CO_2 or CH_4, respectively. In practice, because of equilibria with H_2, reduced carbon remains stable with respect to CH_4 under geologically relevant fO_2 conditions. The degree of dissociation into CO and CO_2 is likewise small under a broad range of conditions. This is because the conversion of all available reduced carbon to $CO\text{-}CO_2$ commonly requires prohibitively high activities of O_2 at sub-solidus temperatures. From a thermodynamic perspective, the abundance of reduced carbon - in diverse rock types – is hence unsurprising.

The graphite stability field expands with pressure. With increasing temperature, reduced carbon-fluid equilibria are increasingly in favour of the fluid phase (‘degassing’), causing amounts of reduced carbon to decrease and the stability field to shrink with respect to solid-state oxygen buffers. The continued ability to provide reduced carbon buffering capacity depends on the amount of carbon, $\sum C$, present in the

system. Evidently, reduced carbon is unstable under highly oxidized conditions, such as provided by assemblages in some haematitic (≈ 'MH' buffer) banded iron-formations ('BIFs'). This may account for the paucity of organic matter in these and other oxidized sediments of controversial biogenicity.

3. Thermodynamic Behaviour of C-O-H Fluids

An overview of the behaviour of C-O-H fluids and the stability of reduced carbon, which are well understood (Connolly, 1995; Holloway, 1984; Huizenga, 2001), is called for. The ternary C-O-H diagram (Figure 3) lends itself well to this purpose.

3.1. Binary and Subcritical Behaviour

As pointed out by Holloway (1984), in the presence of reduced carbon at pressures above $P \approx 300$ bars and temperatures around $T \approx 400$ °C, supercritical C-O-H fluids will consist of either CH_4-H_2-H_2O mixtures or CO_2-CO-H_2O mixtures. Schematically, this situation arises when the reduced carbon saturation isotherm intersects with the CH_4-H_2O or CO_2-H_2O binary, respectively (see T = 400 °C isotherm, Figure 3). At these lower temperatures, fluid equilibria dictate that either H_2/CH_4 or CO/CO_2 ratios are exceedingly low. Any isotopes of carbon in the fluid phase interacting with reduced carbon thus effectively become restricted to a single species, either CH_4 or CO_2. Further consideration of C-O-H fluid behaviour below the binary intersection temperature is relevant here only in so far as it affects the relative amount of reduced carbon precipitating in the system.

Below $T \approx$ 400 °C, CH_4-H_2O fluids gradually undergo unmixing into two separate subcritical CH_4-rich and H_2O-rich phases (Price, 1979). Below ~275 °C, CO_2-H_2O fluids similarly undergo unmixing, into CO_2-rich- and H_2O-rich- phases (Takenouchi and Kennedy, 1964). Unmixed phases become increasingly pure with lower temperatures. Reduced carbon precipitation will still be largely controlled through reduced carbon-CH_4-H_2O-O_2 or reduced carbon-CO_2-H_2O-O_2 equilibria, or an externally imposed oxygen buffer, as the case may be.

Although fluid unmixing may exert some effect on the isotopic equilibrium fractionation with reduced carbon, such considerations become secondary in light of the increasing tendency towards isotopic disequilibrium at these lower temperatures.

3.2. General Supercritical Behaviour

The coincidence of the C-O-H fluid composition with the reduced carbon saturation isotherm described above is a special case. More generally, the molar fractions of CO_2, H_2O, O_2, CO, H_2 and CH_4 are variably fixed in the fluid, depending on constraints placed on the system due to the geological environment. In the case of a single supercritical fluid, three different scenarios can be envisaged under specified *P*, *T* conditions: (i) a fluid whose composition falls outside the stability field of reduced carbon, and is not externally buffered – in which case the relative proportions of species are set by the fluid equilibria themselves; (ii) a fluid whose composition falls outside the stability field of reduced carbon, but is externally buffered; and (iii) a buffered fluid whose composition falls within the stability field of reduced carbon.

3.2.1. Unbuffered Supercritical Fluids

In a system consisting of a single unbuffered supercritical C-O-H fluid, only one phase is present and the system consequently enjoys four degrees of freedom. Hence, in addition to *P* and *T*, the molar proportions of any two of the fluid species must be specified to fix all the others. Consequently, constraints on the isotopic behaviour exhibited by carbon within these fluids can only be sought in their source (e.g. ultramafic versus acidic volcanism). This scenario, though rare, may arise during the passage of a hydrothermal fluid through 'oxidatively-unreactive' lithologies, such as cherts (cryptocrystalline SiO_2). In practice, the presence of small amounts of metal oxides and/or sulfides (particularly combinations of pyrrhotite, pyrite, magnetite and haematite) sets constraints on fO_2 in all but the purest of cases.

In accordance with the controls on reduced carbon stability described above, reduced carbon precipitation may ensue through increased pressures, decreased temperatures, or the external imposition of more reducing conditions.

3.2.2. Buffered Supercritical Fluids, Reduced Carbon Unstable

fO_2-buffers fix fO_2 at a specified P, T. The imposition of such a buffer, expressed in terms of the fugacity of any fluid component in the C-O-H system, restricts the system's degrees of freedom to three. At a specified P, T and fO_2 the system can now be completely described through specification of any remaining compositional variable, such as xH_2O or xCO_2.

3.2.3. Buffered Supercritical Fluids, Reduced Carbon Stable

The behaviour of supercritical fluids within the stability field of reduced carbon naturally merits special consideration. The presence of reduced carbon in the presence of an external buffer adds a strong constraint to the system, reducing its degrees of freedom to two. At a specified P, T and fO_2, the system is invariant, allowing exact determination of the isotopic behaviour of reduced carbon. Figure 4 illustrates calculated 'carbon-saturated' fluid behaviour as a function of temperature at P = 10000 bar.

4. Behaviour of Carbon in Fe-C-O-H System

4.1. Decarbonation of Carbonate

Carbonate minerals whose composition falls within the solid solution space defined by the end-members calcite ($CaCO_3$), dolomite ($CaMg(CO_3)_2$), and siderite ($FeCO_3$) have been common rock-forming minerals throughout geological time. Less common carbonates include magnesite ($MgCO_3$), rhodochrosite ($MnCO_3$) and smithsonite ($ZnCO_3$). The thermal decomposition –or 'decarbonation'– of carbonates can purportedly lead to the precipitation of reduced carbon (Sharp et al., 2003; van Zuilen et al., 2003).

Using a continuous-flow technique within a 3 bar He pressure environment, Sharp et al. (2003) reported the commencement of decarbonation at 720, 600 and 450 ºC for calcite, dolomite and siderite respectively. Higher pressures can be expected to require higher decomposition temperatures, as univariant decarbonation curves have a positive slope in *P-, T-* space (e.g. Kerrick, 1974). Because the potential for isotopic fractionation is limited at the higher decarbonation temperatures required for carbonates outside the Fe-C-O-H system, only the decarbonation of siderite need be considered here.

The decarbonation of siderite has been studied by numerous workers (French, 1971; French and Eugster, 1965; French and Rosenberg, 1965; Frost, 1979; Goldsmith et al., 1962; McCollom, 2003; McCollom, 2004; Mel'nik, 1982; Rosenberg, 1967; Sharp et al., 2003; Weidner, 1968; Weidner, 1972; Yui, 1966). Within the stability field of reduced carbon, the reaction proceeds to form iron oxide:

$$6\ FeCO_3 = 2\ Fe_3O_4 + 2\ x\ CO + 4\ y\ CO_2 + (6 - 2\ x - 4\ y)\ C + (5 - x - 4\ y)\ O_2 \qquad (4)$$

Here, the molar coefficients x and y are determined through reduced carbon-vapor equilibration in the C-O system, $C + O_2 = CO_2$ and $C + 0.5\ O_2 = CO$.

In the system reduced carbon-C-O, all compositional fluid variables (xCO_2, xCO and xO_2) are fixed at a specified *P, T*. We can exploit this fact to determine the amount of reduced carbon precipitated as a function of *P, T* by solving for *x, y* in reaction (04). Above the decarbonation temperature, ~1 mole of reduced carbon and ~5 moles of CO_2 are generated for every 6 moles of siderite decarbonated (Figure 5). With increasing temperature, the CO/CO_2 ratio of the evolved fluid increases, while the amount of reduced carbon precipitated decreases up to the limit of its stability.

The foregoing assumes that fO_2 is not externally buffered above the stability of graphite. If this were the case, the relative amounts of CO_2, CO and O_2 produced would now be determined by the equilibrium $CO + 0.5\ O_2 = CO_2$. The assemblage siderite – magnetite - C-O-fluid (or, at $fO_2 > fO_2^{MH}$, the assemblage siderite - haematite - C-O-fluid) is divariant.

5. Isotopic Behaviour of Carbon in Fe-C-O-H Systems

5.1. Parameterizing the Isotopic Behavior of Individual Compounds

The β-factor, or 'reduced isotopic partition function ratio', is a useful parameter when studying the effect of metamorphism or metasomatism on isotopic exchange. β-factors parameterize the isotopic behavior of individual substances, allowing for the calculation of the overall equilibrium fractionation effect α in reactions involving isotopic interaction between two or more substances. Explicitly, the isotope fractionation factor $\alpha_{A\text{-}B}$ between two substances A and B undergoing equilibrium exchange is equal to the ratio of their individual β-factors β_A and β_B:

$$\alpha_{A-B} = \frac{\beta_A}{\beta_B} \qquad \text{or} \qquad \ln \alpha_{A-B} = \ln \beta_A - \ln \beta_B \tag{5}$$

The alpha factor α allows determination of the isotopic ratio of two species. The isotopic ratio for a species A, R_A, can also be expressed in the customary δ_A notation:

$$\alpha_{A-B} = \frac{R_A}{R_B} \qquad R_A = \frac{(\frac{^{13}C}{^{12}C})_A}{(\frac{^{13}C}{^{12}C})_{std}} \qquad \delta^{13}C_A = (R_A - 1) \cdot 1000 \tag{6}$$

Here, subscript 'std' refers to the known isotopic ratio in a laboratory standard, such Peedee Belemnite ('PDB'). Equations (05) and (06) are applicable to all carbon species in the system Fe-C-O-H under consideration. The β-factors for reduced carbon, CO_2, CO, CH_4 and siderite are compared in Figure 6. The distinctly higher β-factors exhibited by CO_2 result in its isotopic enrichment relative to CH_4 and CO.

The effect of pressure on isotopic fractionation is usually taken to be negligible (Chacko et al., 2001), as studies at geologically relevant pressures have consistently revealed negligible (<0.1‰) pressure-induced corrections (e.g. Clayton et al., 1975; Hamann et al., 1984; Joy and Libby, 1960). In the case of graphite, however, Kharlashina and Polyakov (1992) noted that β-values exhibit an anomalously large pressure-dependence, on the order of 1‰ over 10 kbar. From a kinetic perspective, it is well known that elevated pressures lead to enhanced isotopic exchange rates (Clayton

et al., 1975; Matsuhisa et al., 1979; Matthews et al., 1983a; Matthews et al., 1983b; Matthews et al., 1983c).

5.2. Isotopic Equilibration of Reduced Carbon with C-O-H fluids

In the presence of C-O-H fluids, reduced carbon isotopically interacts with fluid-phase CO_2, CO and CH_4. Under the assumptions specified above, coupling of the thermodynamic- (xCO_2, xCO and xCH_4) and isotopic- (βCO_2, βCO, βCH_4 and $\beta redC$) behaviour allows calculation of $\delta^{13}C_C$ as a function of P, T and fO_2:

$$\alpha_{C\text{-}fluid} = (\beta CO_2/\beta redC)\cdot xCO_2 + (\beta CO/\beta redC)\cdot xCO + (\beta CH_4/\beta redC)\cdot xCH_4 \quad (7)$$

$$R_{redCs} = \alpha_{C\text{-}fluid} \cdot R_{fluid}$$

$$\delta^{13}C_{redC} = (R_{redC} - 1)\cdot 1000 \quad (8)$$

Here, R_{fluid} and R_C refer to the isotopic ratios in the bulk fluid and reduced carbon, respectively. Figure 7(a-c) shows the isotopic fractionation of reduced carbon equilibrating with C-O-H fluids in fO_2 - T space at three different pressures.

5.3. Isotopic Equilibration in Carbonate-Reduced Carbon Systems

The carbonate-reduced carbon system has received considerable attention because of its potential use as a geothermometer. Theoretical (Bottinga, 1969; Chacko et al., 1991; Golyshev et al., 1981; Polyakov and Kharlashina, 1995a), empirical (Dunn and Valley, 1992; Kitchen and Valley, 1995; Morikiyo, 1984; Valley and Oneil, 1981; Wada and Suzuki, 1983) and laboratory (Scheele and Hoefs, 1992) methods have been employed to study the temperature-dependence of isotope equilibrium fractionation within the calcite-graphite system (Figure 8a, b). The temperature-dependence of the dolomite β-factor (Golyshev et al., 1981; Wada and Suzuki, 1983) and siderite β-factor (Carothers et al., 1988; Golyshev et al., 1981; Jimenez-Lopez and Romanek, 2004; Zhang et al., 2001) have also been investigated. Carbonate β-factors roughly increase with decreasing cation radius.

Significant divergence exists between studies focusing on lower temperatures ($270 < T < 650$ °C) and those addressing higher temperatures ($T > 650$ °C). Theoretical calculations are consistent with the data at high temperatures, suggesting that the deviation of low-temperature natural sample data from theory results from incomplete equilibration and kinetic effects at depressed temperatures.

Isotopic carbonate-reduced carbon equilibria are also important to geobiologists studying metamorphosed rocks (Figure 9). Isotope re-equilibration between reduced carbon and carbonate during metamorphism is commonly invoked, for example, to explain the $\delta^{13}C$ distribution in the 3.8 Ga Isua Supracrustal Belt and Akilia Gneiss of southwest Greenland (Mojzsis et al., 1996; Mojzsis and Harrison, 2000; Schidlowski, 1988; Schidlowski, 2001; Schidlowski et al., 1979).

In a simple closed system, the bulk $\delta^{13}C$ is time-invariant, and carbon isotope systematics can easily be constrained using the mass balance equations:

$$\delta^{13}C_{bulk} = \delta^{13}C^{i}_{redC}\, X_{redC} + \delta^{13}C^{i}_{carb}\, X_{carb}$$
$$= \delta^{13}C_{bulk} = \delta^{13}C^{f}_{redC}\, X_{redC} + \delta^{13}C^{f}_{carb}\, X_{carb} \qquad (9)$$

Here, the superscripts *i* and *f* refer to the initial and final, or pre- and post- metamorphic states respectively; the subscripts '*bulk'*, *'C'* and '*carb'* refer to the combined, reduced carbon and carbonate components, respectively; X is the molar fraction of a given component (capitalized to distinguish it from fluid compositions discussed previously) such that $X_{redC} + X_{carb} = 1$. It should be noted that for realistic geological systems, the molar fractions X_{redC} and X_{carb} are unlikely to be time-invariant due to processes such as the interaction with graphitic fluids and CO_2 degassing of carbonates. These complications are considered in Section 5.5 below.

Equations (09) can be recast into a form incorporating $\Delta_{carb\text{-}C}\,(T)$, the isotopic fractionation factor between carbonate and organic carbon:

$$\delta^{13}C_{bulk} = \delta^{13}C^{f}_{redC} + \Delta_{carb\text{-}C}\, R_x\, (1 + R_x)^{-1} \qquad (10)$$

Here, the important variable R_x is the molar ratio X_{carb} / X_{redC}. The isotopic behaviour in a system governed by equation (10) is illustrated in Figure 10.

5.5. Carbon Isotopic Fractionation During Decarbonation

The process of decarbonation can ostensibly produce graphite *de novo* at temperatures as low as $T \approx 450$ ºC. Good experimental data on the isotopic fractionation during the decarbonation of different carbonate minerals is scarce. In one study, the measured carbon isotope fractionation between calcite or dolomite and evolved CO_2 (from which the isotopic evolution of reduced carbon may be calculated) was negligible, whereas the $\delta^{13}C$ of evolved CO_2 during laboratory decarbonation of siderite increased as a function of reaction process from an initial + 1 ‰ to a maximum of +5 ‰ (Sharp et al., 2003). These findings agree with calculations of carbonate-reduced carbon-CO_2 equilibration (Figure 11). In the absence of more or contradictory experimental data, therefore, equilibration calculations will be used to examine the isotopic evolution of reduced carbon in systems undergoing carbonate decarbonation.

5.5.1. Closed System Decarbonation

During complete closed system decarbonation, the isotopic evolution of reduced carbon will equilibrate with evolved CO_2 and CO:

$$\delta^{13}C_{FeCO_3} = \delta^{13}C_{CO_2} \cdot xCO_2 + \delta^{13}C_{CO} \cdot xCO + \delta^{13}C_{redC} \cdot xredC \tag{11}$$

$$\alpha_{C\text{-}fluid} = (\beta CO_2/\beta redC) \cdot xCO_2 + (\beta CO/\beta redC) \cdot xCO$$

$$\delta^{13}C_{fluid} = \frac{\delta^{13}C_{CO_2} \cdot xCO_2 + \delta^{13}C_{CO} \cdot xCO}{xCO_2 + xCO} \tag{12}$$

$$R_{CO_2} = R_{redC} \frac{\beta_{CO_2}}{\beta_{redC}} \quad \text{and} \quad R_{CO} = R_{redC} \frac{\beta_{CO}}{\beta_{redC}} \tag{13}$$

$$R_{redC} = \frac{R_{FeCO_3} \cdot \beta_{redC} \cdot x_{redC}}{\beta_{redC} \cdot x_{redC} + \beta_{CO_2} \cdot x_{CO_2} + \beta_{CO} \cdot x_{CO}} \tag{14}$$

Reduced carbon produced through this mechanism will be isotopically depleted relative to precursor carbonate by between 2 and ~8 ‰, depending mostly on the

temperature of peak metamorphism (Figure 12). Severely depleted (< -15 ‰ relative to precursor carbonate) reduced carbon cannot be produced through this mechanism.

5.5.2. Open System Decarbonation

Both organic matter and carbonate may undergo open-system devolatilization. Unlike closed-system isotopic equilibration, the isotopic signature of the remnant carbon reservoir will evolve over time. Open-system devolatilization reactions follow a Rayleigh distillation curve:

$$\delta^{13}C^{final} = (\delta^{13}C^{initial} + 1000) \cdot f^{(\alpha - 1)} - 1000 \quad (15)$$

Here, f refers to the fraction of carbon remaining following devolatilization, $0 \leq f \leq 1$; and α refers to the fractionation factor between the released volatiles and the devolatilizing carbon pool.

For the open-system devolatilization of carbonate, the isotopic signature of carbonate itself evolves with time:

$$\delta^{13}C_{carb} = (\delta^{13}C^{i}_{carb} + 1000) \cdot f^{(\alpha - 1)} - 1000 \quad (16)$$

It is assumed that the precipitated reduced carbon equilibrates isotopically with remnant carbonate, such that $R_{redC} = R_{carb} \frac{\beta_{redC}}{\beta_{carb}}$. This seems a reasonable assumption, given that thermodynamics constrain decarbonation temperatures above ~450 °C where solid-solid isotope exchange is unlikely to suffer from severe disequilibrium effects. The real difficulty, rather, lies in determining the fractionation factor α that governs the isotopic composition of the released volatiles.

In the laboratory, graphite is produced even if a constant He atmosphere is maintained. The devolved fluid is oversaturated in CO with respect to CO_2 and reduced carbon, causing precipitation of the latter. This suggests that, even under these extremely dynamic artificial open-system conditions, thermodynamic equilibration is partly occurring. Figure 13(a-c) shows the results of calculations on the final isotopic

signature of *de novo* graphite assuming perfect isotopic and thermodynamic equilibrium with devolved CO-CO_2 fluid.

As under closed-system conditions, the production of non-biological reduced carbon with a severely depleted isotopic signature is predicted to occur only at low pressures ($P < 1000$ bar).

In the case of the devolatilization of abiotic hydrocarbon, $C_nH_mO_l$, both the geological environment and the hydrocarbon composition affect the relative amounts of CO_2, CO and CH_4 in the evolved gas. Unfortunately, little is known about the individual isotopic behaviour of more complex hydrocarbons (e.g. Chung et al., 1988). In consequence, we assume that the isotopic properties of graphite hold for kerogen. The isotopic evolution of a devolatilizing organic carbon reservoir governed by the form of equation (18) is illustrated in Figure 14.

At high CO_2/CH_4 ratios, and in the absence of carbonate, this mechanism can theoretically lead to reduced carbon as fractionated as $\Delta\delta^{13}C_{redC}$ = -40 ‰ relative to its pre-devolatilization signature.

6. Discussion

6.1. Summary

Under the explicit assumption of complete isotopic equilibrium and C-O-H fluid behaviour dictated by Modified-Redlich-Kwong (MRK) equation of state, a detailed investigation of the non-biological production of isotopically depleted reduced carbon from an isotopically heavy precursor reservoir of magmatic carbon and/or carbonate carbon in the system Fe-C-O-H was conducted. Starting with a C-O-H fluid reservoir isotopically representative of a magmatic origin ($\delta^{13}C_{fluid} \approx$ -5 ‰), the production of reduced carbon bearing a signature within the range of biological processes ($\delta^{13}C_{final} <$ -15 ‰) is restricted to very reducing conditions: over 8 log units below fO_2^{QFM} at geologically relevant pressures. With increasing temperature, the amount of carbon precipitated decreases but endures little isotopic shift.

The production of reduced carbon that accompanies the decarbonation of common rock-forming carbonates (dolomite, calcite and siderite) is frequently put forward as a source for isotopically reduced carbon. The nature of the carbonate cation has a significant effect on its isotopic behaviour, particularly at low temperatures. However, with the exception of siderite, decarbonation occurs at temperatures prohibitively high for significant isotopic fractionation. The decarbonation of an isotopically heavy carbon reservoir representative of marine siderite ($\delta^{13}C_{carb} \approx 0$ ‰) within a closed equilibrating system is not conducive to the production of isotopically light reduced carbon ($\delta^{13}C_{final} < -15$ ‰). It is worth noting that the geological literature is suspiciously barren of petrological evidence for this mechanism happening outside the laboratory. This author has never encountered evidence for carbonate-derived graphite in metacarbonates.

Replacing the constraint of closed-system equilibrium for one of open-system Rayleigh-style degassing, but conserving the assumption of equilibrium isotopic exchange between carbonate and reduced carbon, does little to improve the potential for isotopically light reduced carbon production under geologically relevant conditions of P, T and fO_2. In fact, equilibrium considerations require that the continued decarbonation of carbonate isotopically enriches, rather than depletes, the reduced carbon produced.

In the absence of carbonate, and at temperatures below 500 °C, open-system Rayleigh-style degassing of graphite-like hydrocarbon material can theoretically give rise to carbon with 'life-like' isotope signatures if high CO_2/CH_4 ratios ($R > 1$) predominate in the devolved gas. However, large fractions ($f > 0.5$ at $T = 300$ °C and $f > 0.9$ at $T = 500$ °C) of precursor hydrocarbon material must be devolatilized for this to occur. Thus, large quantities of pre-existing concentrated non-biological hydrocarbon would be required.

6.2. Conclusion

The production of severely isotopically depleted ($\Delta\delta^{13}C \leq$ -15‰) reduced carbon from an unfractionated carbon pool at isotopic and thermodynamic equilibrium is challenging under conditions relevant to geological systems. Only under exceptional circumstances can commonly invoked processes, such as graphite precipitation from C-O-H fluids and the decarbonation of carbonates, give rise to carbon fractionation incurred during enzymatically-mediated metabolic processes.

The non-biological production of isotopically depleted carbon capable of mimicking a biological isotopic fingerprint, therefore, necessitates conditions of severe disequilibrium - reminiscent of biological systems themselves (e.g. Shock, 1992). For carbon isotopes to acquire their intended utility in biosignature studies, therefore, requires that the operation of disequilibrium processes involving carbonic fluids be incontrovertibly refuted. Unless this precondition is met, isotopically depleted reduced carbon remains, by itself, an unsuitable indicator of primitive biology in highly metamorphosed rocks.

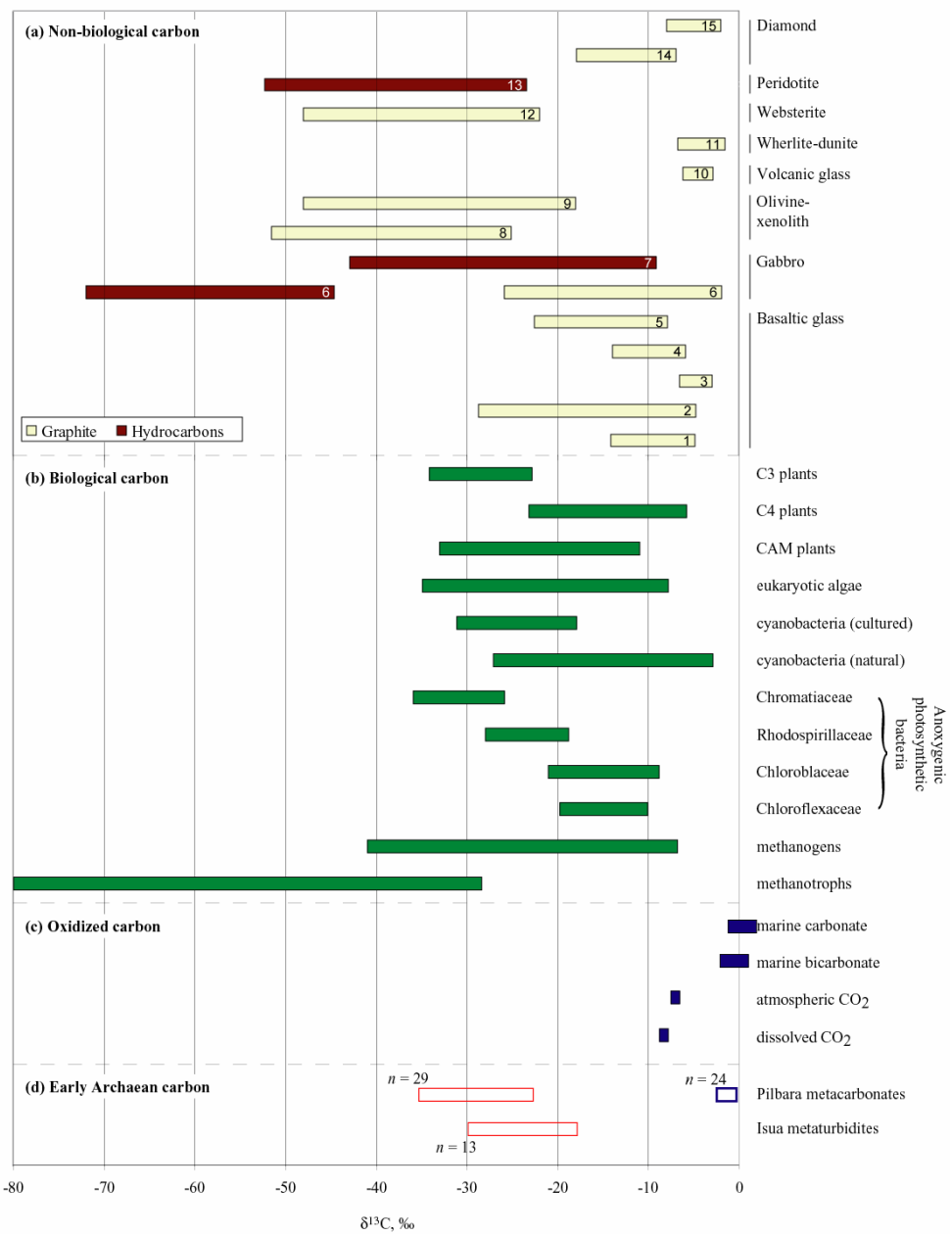

Figure 1: Isotopic fractionation of carbon. (a): Graphite and hydrocarbons hosted in a variety of igenous rocks. Reference numbers in bars: 1. Blank et al. (1993); 2 & 4. Des Marais and Moore (1984); 3. Javoy and Pineau (1991); 5. Mattey et al. (1984); 6 & 7. Kelley and Fruh-Green (1999); 8 & 9. Hoefs (1975); 10. Gerlach and Taylor (1990); 11 & 12. Pineau and Mathez (1990); 13. Sugisaki and Mimura (1994); 14. Swart et al. (1983); 15. Deines (1980). (b): Biological carbon (after Schidlowski, 2001). (c): Atmospheric and marine dissolved carbon. (d): Reduced and carbonate carbon from >3.7 Ga lower-amphibolite-facies metaturbidites from the Isua Supracrustal Belt, Greenland and >3.52 Ga upper-greenschist-facies metasedimentary carbonate from the Pilbara Craton, Australia (Chapter 5, 6, 8).

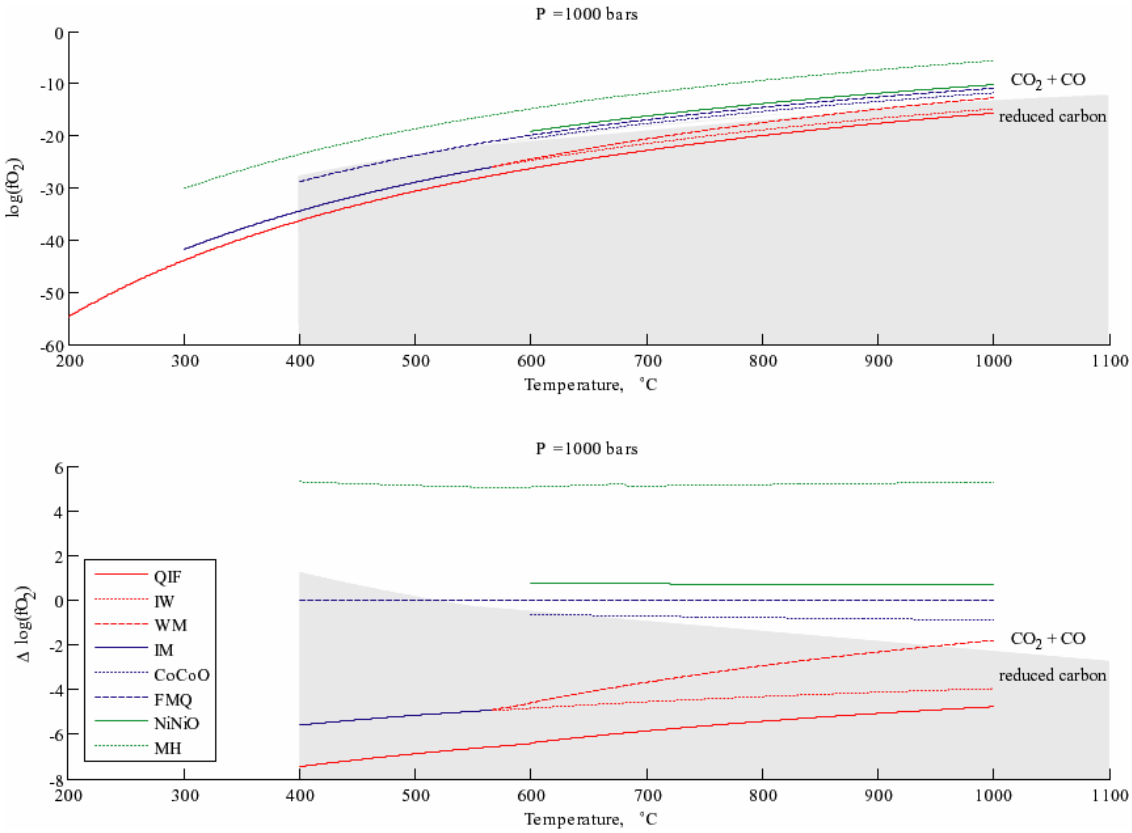

Figure 2: Oxygen buffers and graphite stability plotted in $fO_2 - T$ space. The graphite stability field is shown in grey. (a) A range of common oxygen buffers at P= 1000 bars. (b) Oxygen buffers, at P= 1000 bars, plotted in $\Delta fO_2 - T$ space relative to the FMQ buffer: $\Delta\ log(fO_2) = log(fO_2) - log(fO_2^{FMQ})$. All buffers lie within 6 log units above and 8 log units below the FMQ buffer, corresponding to the oxygen fugacity range considered in this study. Buffer abbreviations used: QIF: Fe2SiO4 = 2Fe + SiO2 + O_2; IW: 2 FexO = 2x Fe + O_2; WM: 2x/(4x-3) Fe3O4 = 6/(4x-3) FexO + O_2; CoCoO: 2 CoO = 2 Co + O_2; FMQ: 2 Fe3O4 + 3 SiO2 = 3Fe2SiO4 + O_2; NiNiO: 2 NiO = 2 Ni + O_2; MH: 6 Fe2O3 = 4 Fe3O4 + O_2. For the QIF and FMQ buffers, the alpha-beta quartz phase transition at T (°C) $\approx 573 + 0.025\ P$ (bar) was taken into account.

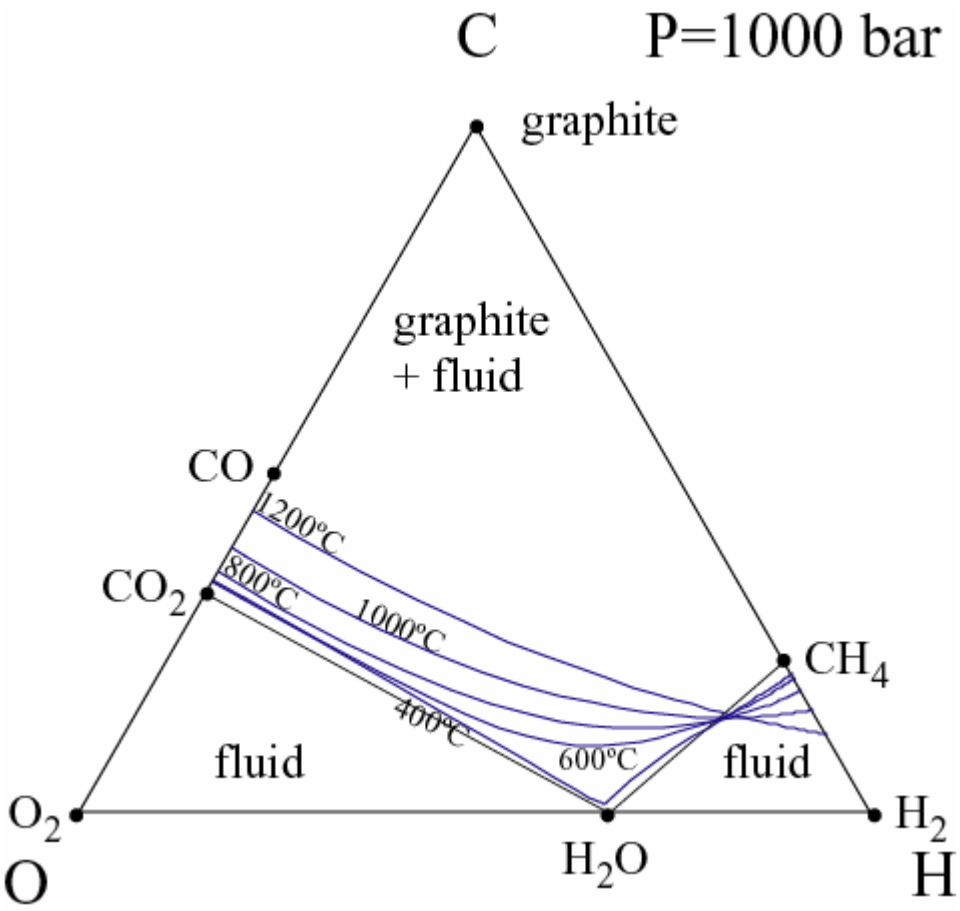

Figure 3: The ternary C-O-H diagram, showing calculated graphite saturation isotherms at T = 400, 600, 800, 1000 and 1200 °C. Note the near-overlap of the isotherms with the CO_2-H_2O and H_2O-CH_4 binary joins at T = 400 °C, and the continued dominance of CO_2 and CH_4 over CO and H_2, respectively, even at elevated temperatures.

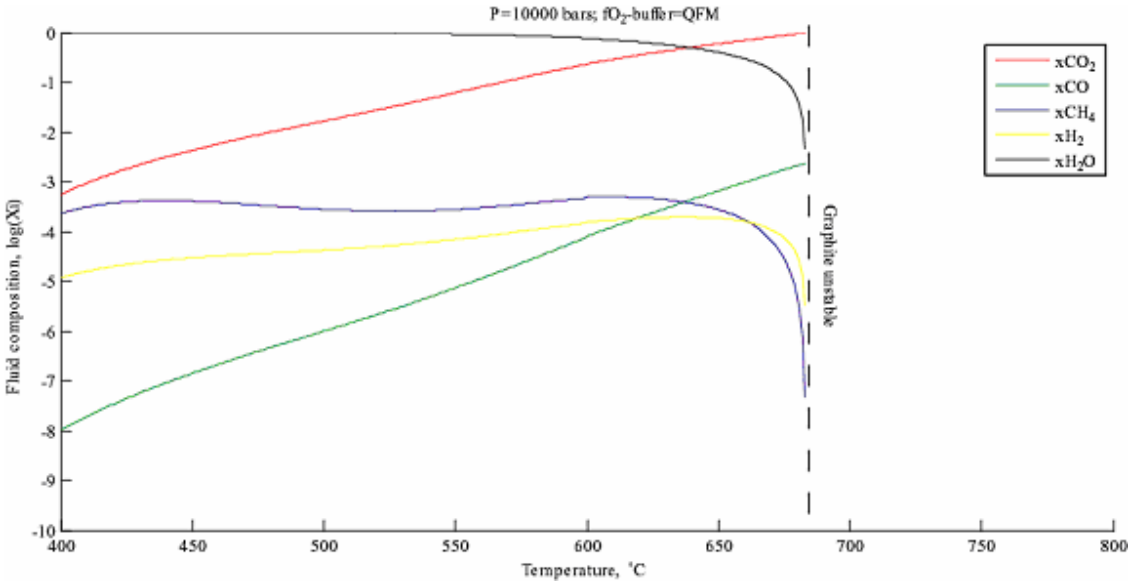

Figure 4: Fugacities of CO_2, H_2O, O_2, CO, H_2 and CH_4 as a function of *P*, *T* and fO_2 in a supercritical graphite-saturated C-O-H fluid.

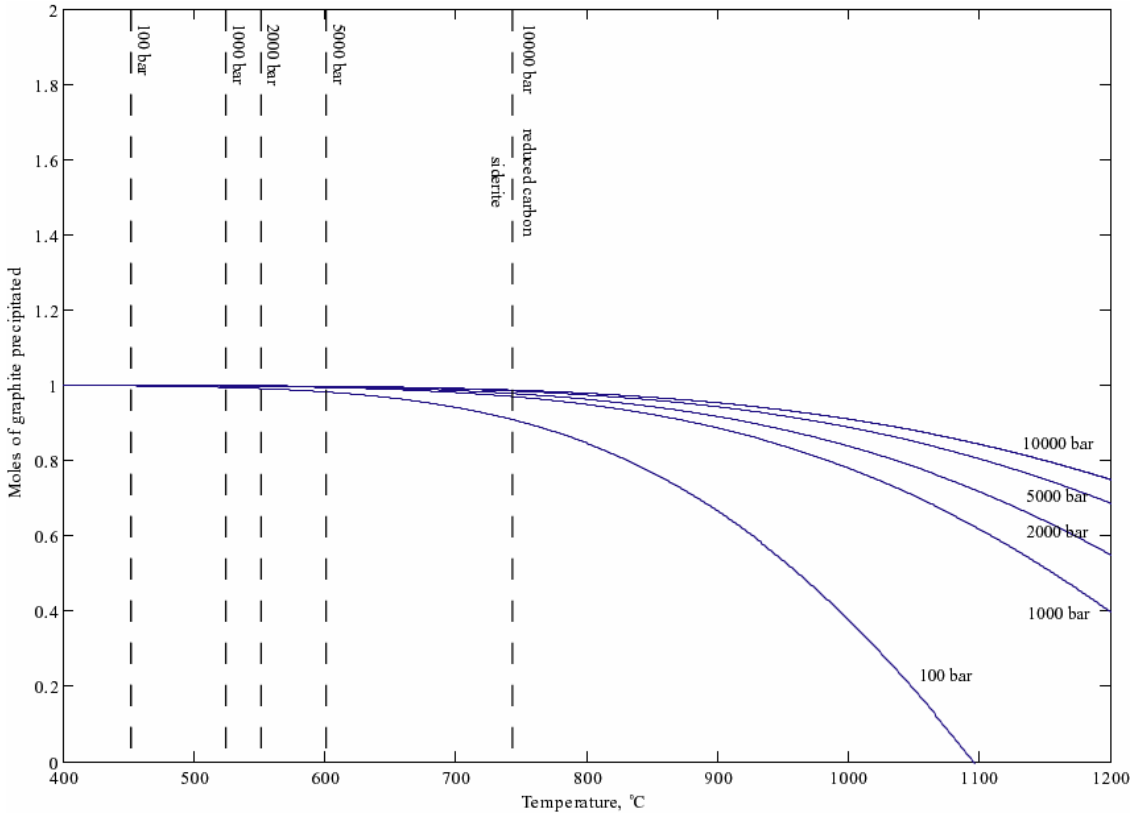

Figure 5: Number of moles of graphite precipitated for every 6 moles of siderite decarbonated as a function of temperature at different pressures, as per reaction (4). Dashed lines indicate stability of siderite at specified pressures. Closed-system equilibrium conditions are assumed.

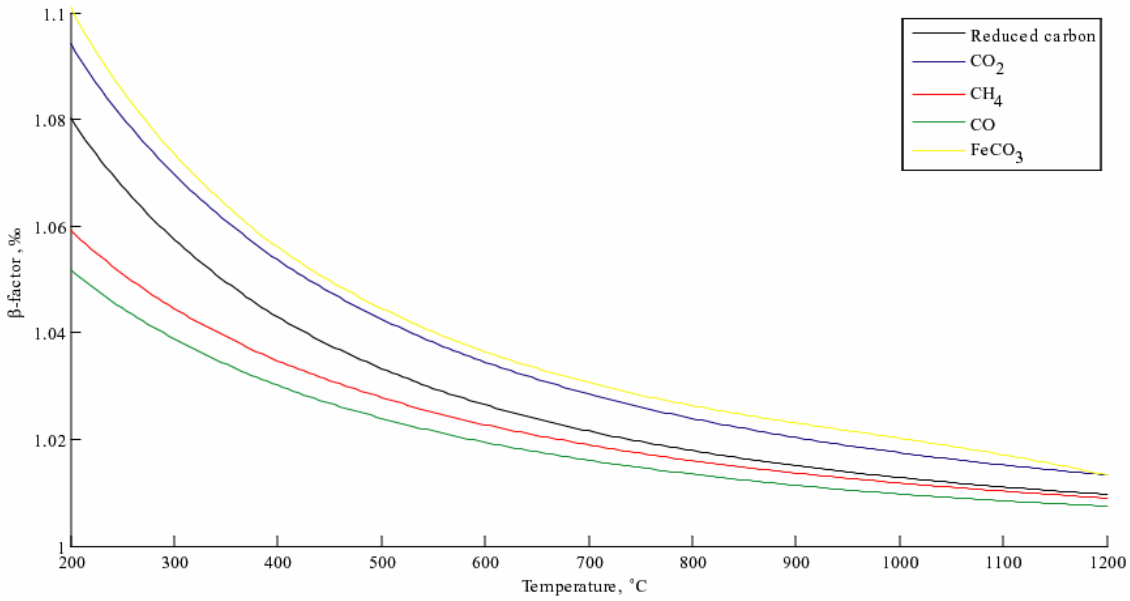

Figure 6: Theoretical β-factors of CO_2, CO and CH_4 as a function of temperature, calculated using thermodynamic and quantum mechanical data for gaseous molecules compiled in (Richet and Bottinga, 1977) with minor amendments proposed by (Horita, 2001). Note the deviating behaviour exhibited by 'heavier' CO_2 relative to the more reduced species CH_4 and CO.

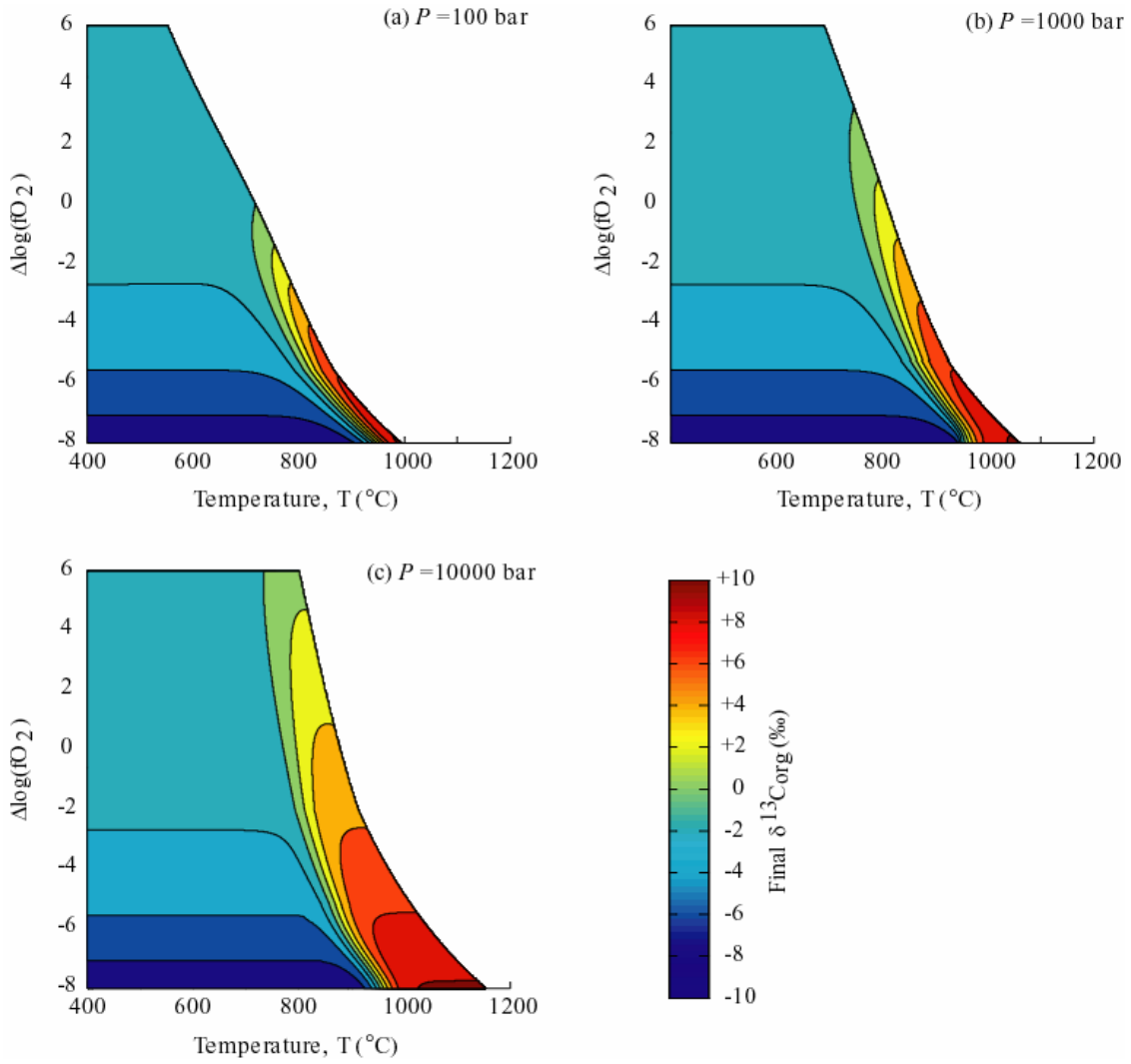

Figure 7: Contour plots showing the isotopic fractionation of reduced carbon equilibrating with C-O-H fluid (with $\delta^{13}C_{fluid}$ = -5 ‰) in fO_2 - T space at P = (a) 100, (b) 1000 and (c) 10000 bars.

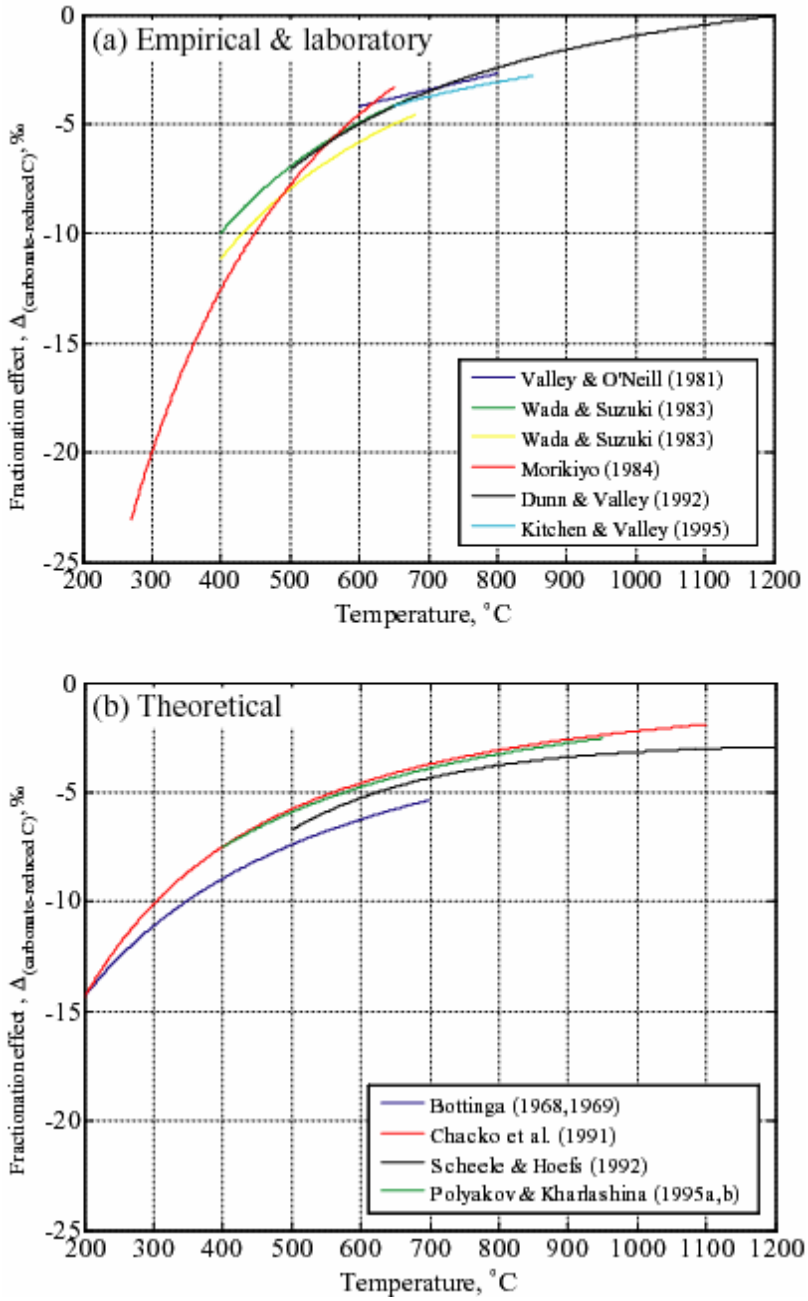

Figure 8: (a): Theoretical (**blue** curve – Bottinga (1968; 1969); **green** curve – Chacko et al. (1991); **red** curve – Polyakov and Kharlashina (1995a; 1995b)) and laboratory (**black** curve – Scheele and Hoefs (1992)) results for carbon isotope fractionation within the calcite-graphite system. (b): Emperical results for carbon isotope fractionation within the calcite-graphite system. **Blue** curve – Valley and O'Neil (1981); **green** curve – Wada and Suzuki (1983); **yellow** curve – dolomite, Wada and Suzuki (1983); **red** curve – Morikiyo (1984); **black** curve – Dunn and Valley (1992); **cyan** curve – Kitchen and Valley (1995). All curves calculated using cubic spline fitting.

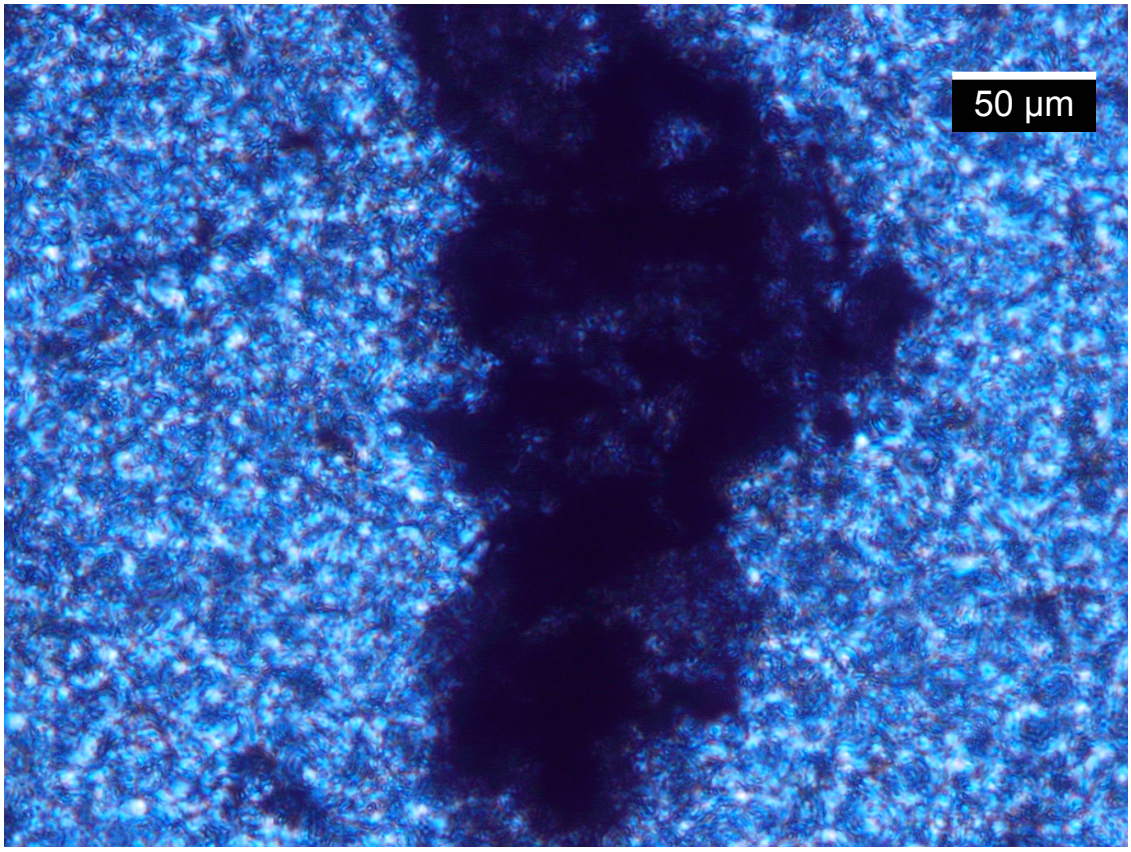

Figure 9: Thin-section photographs of reduced carbon in thermodynamic equilibrium with carbonate. Amoebal graphitic kerogen enclosed in ferruginous dolomite in the greenschist-facies ~3.5 Ga Strelley Pool Chert, Warrawoona Group, Pilbara Craton, Western Australia.

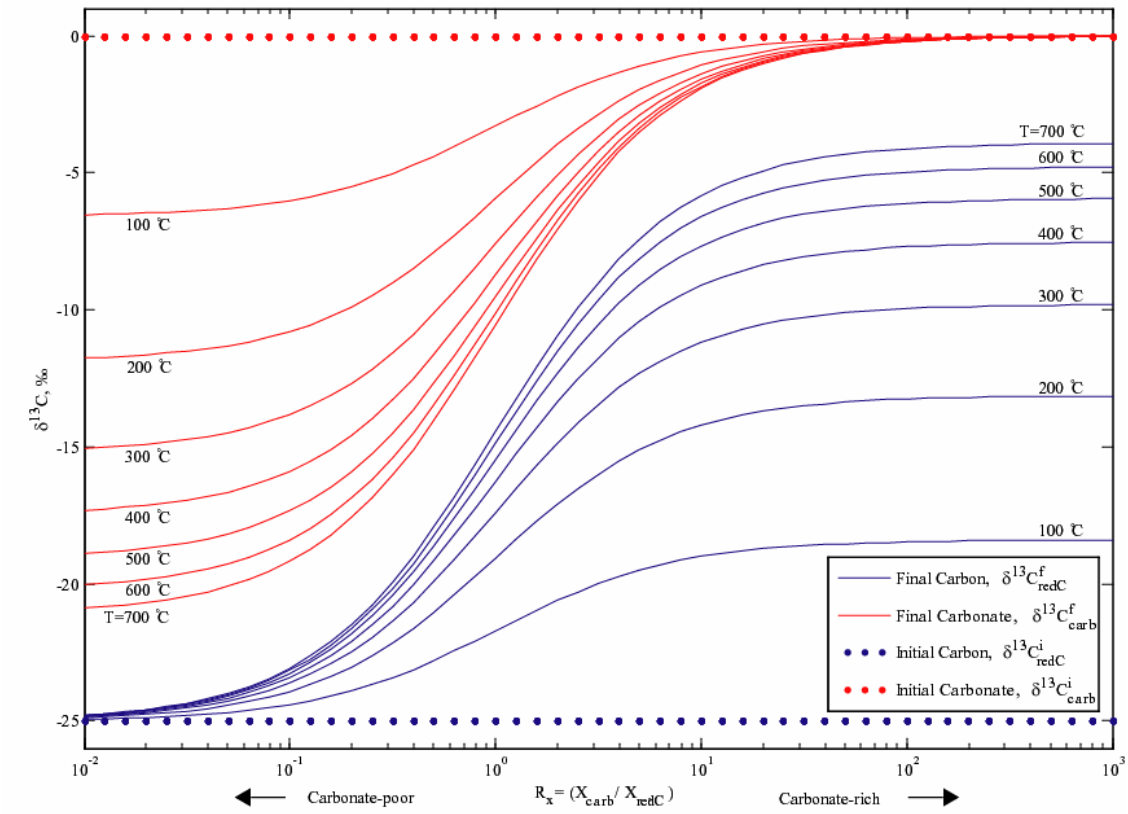

Figure 10: Modelled carbon isotope ratios resulting from equilibrium closed-system interaction between reduced carbon (blue curves) and carbonate (red curves) at different temperatures (100 < T < 700 °C). Non-equilibrium invalidates the lower-temperature calculations. Dotted lines indicate initial isotope ratios, set at $\delta^{13}C^{i}_{C}$ = -25 ‰ and $\delta^{13}C^{i}_{carb}$ = 0 ‰. Higher temperatures tend to drive the isotope ratios of the two distinct carbon reservoirs together. Note the importance of the R, the ratio of carbonate, X_{carb}, to organic carbon, X_C, in determining the final observed $\delta^{13}C^{f}_{C}$.

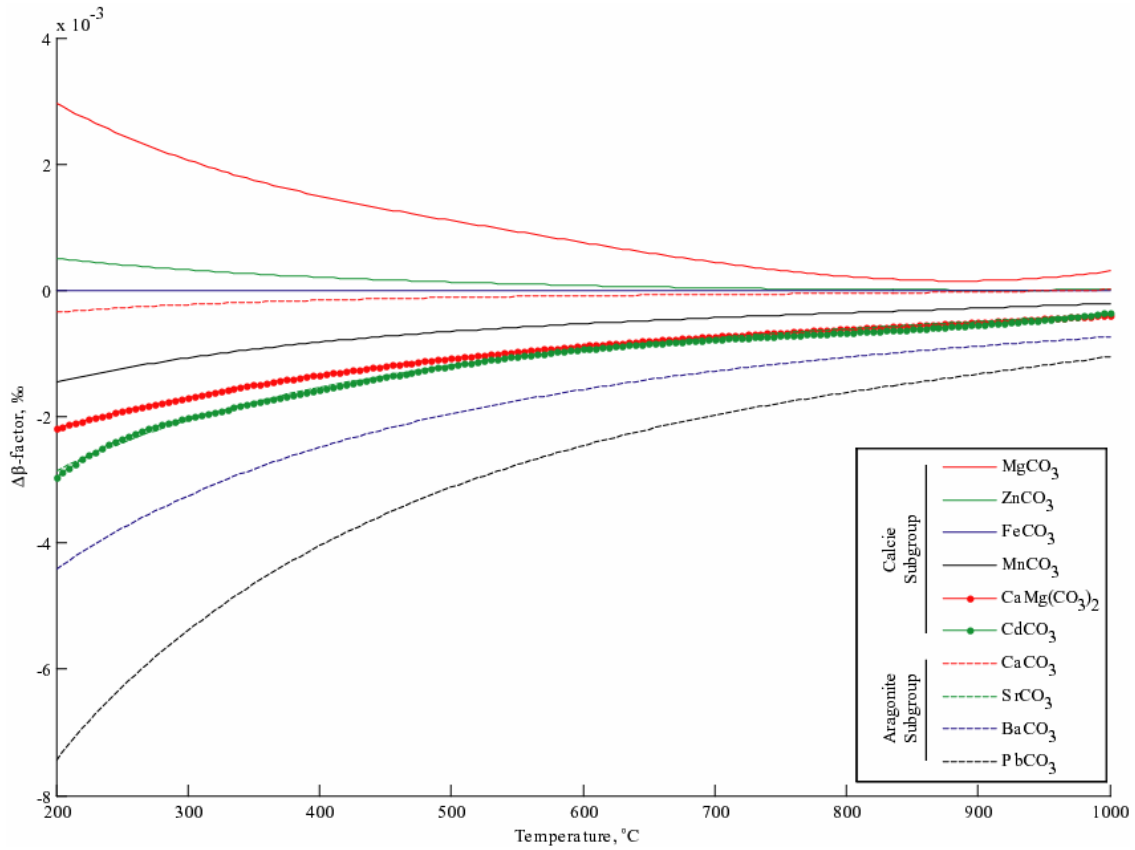

Figure 11: β-factors for a variety of carbonates in the calcite and aragonite subgroups plotted relative to siderite ($FeCO_3$) as a function of temperature. β-factors decrease with increasing metal^{++} cation radius. Plot based on cubic spline fitting of data in Golyshev et al. (1981).

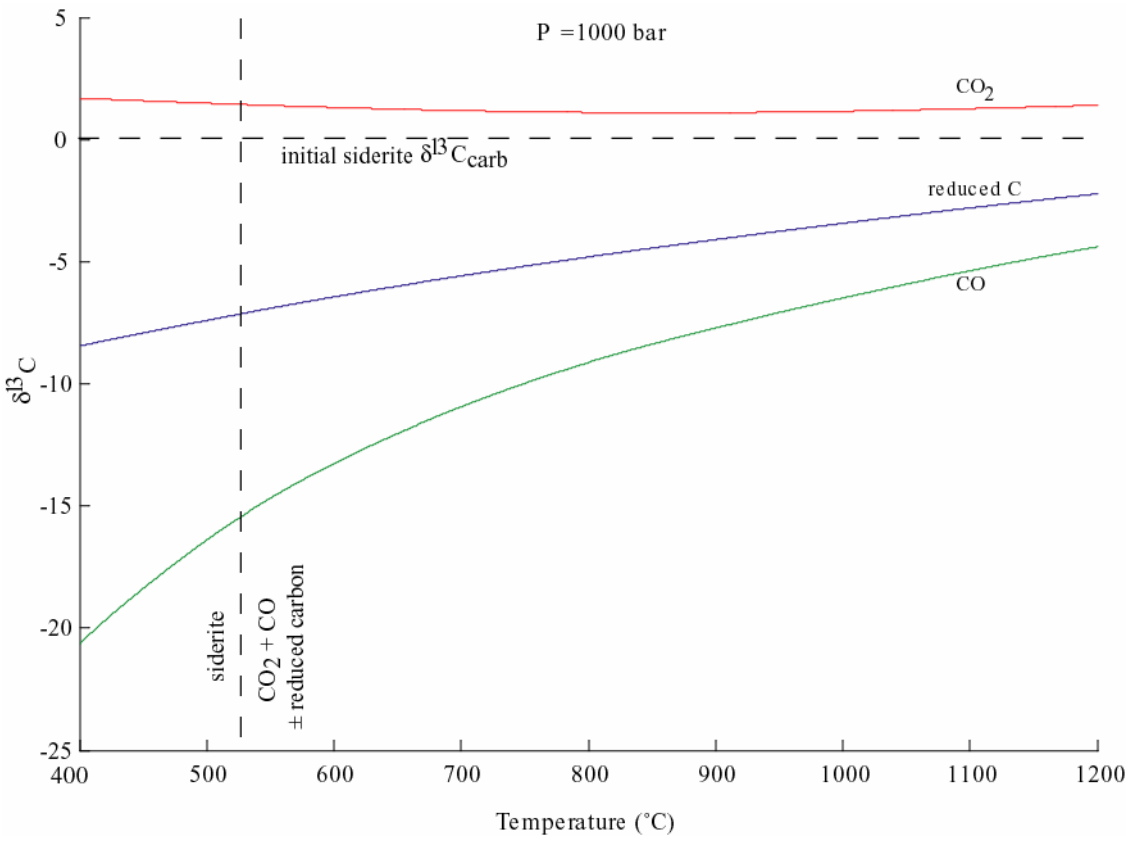

Figure 12: Modelled carbon isotope ratios in the reaction products of closed-system equilibrium decarbonation of siderite (initial $\delta^{13}C^{i}_{carb}$ = 0 ‰, horizontal dashed line) as a function of temperature at P = 1000 bar. Vertical dashed line indicates maximum temperature of siderite stability at the specified pressure.

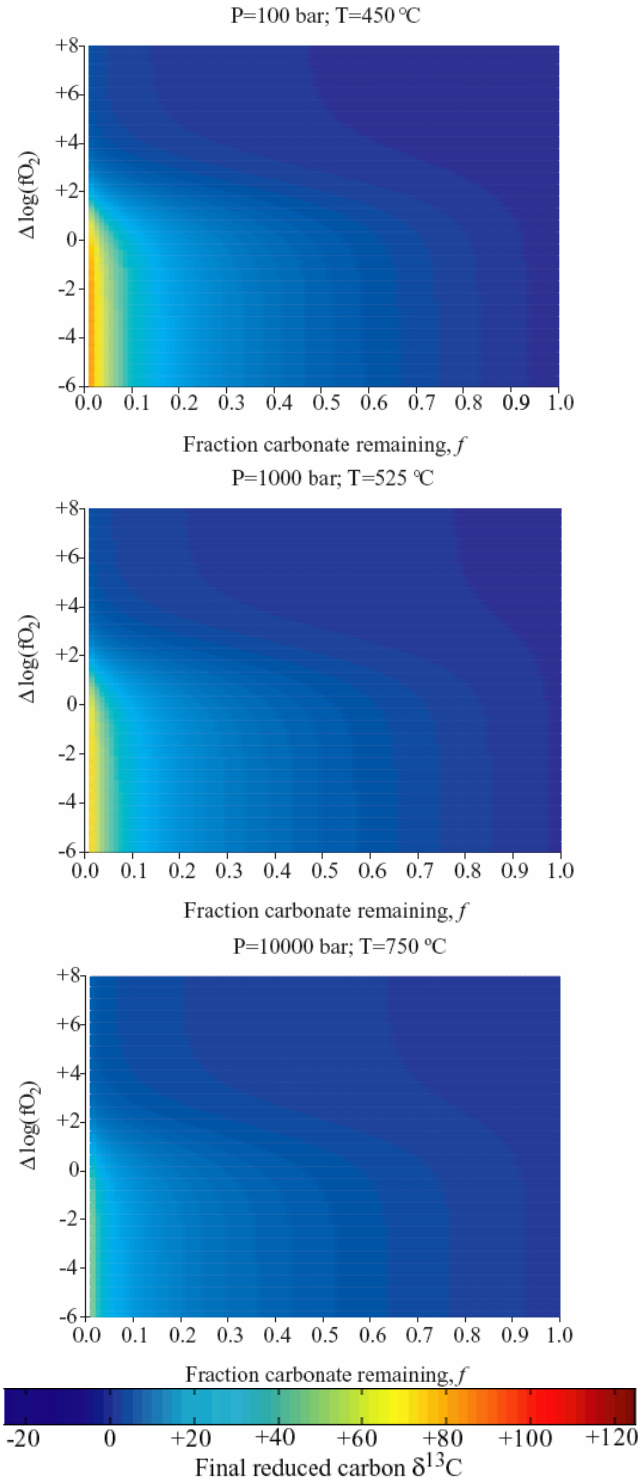

Figure 13: Contour plots of isotopic composition of carbon produced through open-system equilibrium decarbonation of siderite (initial $\delta^{13}C^{i}_{carb}$ = 0 ‰) as a function of the ratio CO_2 to CO in the emitted gas (R_c), and the fraction of carbonate remaining (f). Calculations performed along the univariant decarbonation curve of siderite.

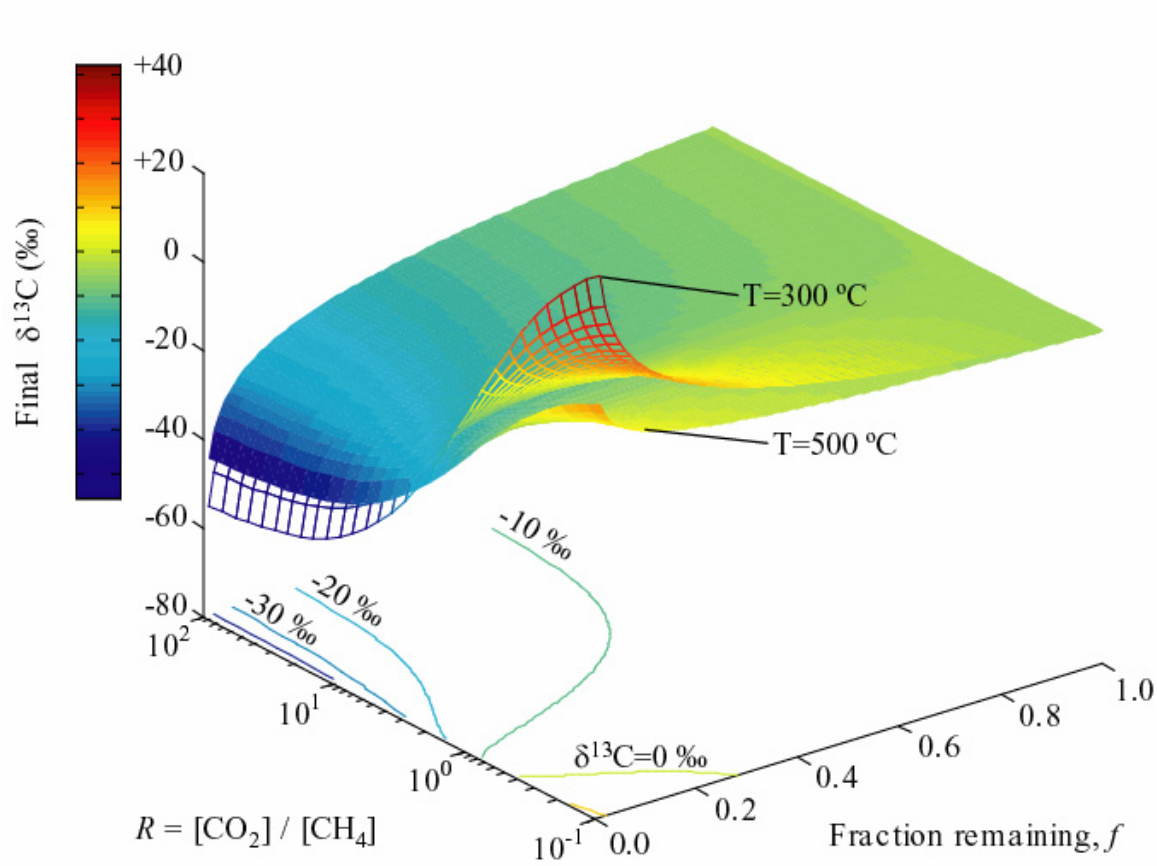

Figure 14: Isotopic fractionation incurred from open-system devolatilization (Rayleigh-type distillation) of graphite-like organic hydrocarbons with an initial isotope signature $\delta^{13}C$ = -5 ‰. The final isotope signature of remaining reduced carbon is plotted as both a function of R_c, the ratio CO_2 to CH_4 in the emitted gas, and f, the fraction of hydrocarbon remaining following devolatilization. The transparent and filled surfaces represent devolatilization at temperatures T = 300 and 500 ºC respectively. Labeled projected 10‰ contours show values in R-f space giving rise to remnant reduced carbon with $\delta^{13}C$ = -40 to + 10‰ for T = 500 ºC.

Table 1: Mixing parameters and thermodynamic constants used in Modified Redlich-Kwong (MRK) equation of state, as proposed by Frost and Wood (1995).

Molecule	**Moment (Debyes)**	***a*** **(at T=1000 K)**	***b*** **(cm^3 $mole^{-1}$)**
H_2	0.00	3.6	15.2
O_2	0.00	17.2	22.1
CH_4	0.02	31.6	29.7
CO_2	0.18	83.0	29.7
CO	1.38	17.0	27.3
H_2O	1.85	88.0	14.6

Table 2: Values taken on by $a_{i,j}$ ($i \neq j$) in the expansion of the MRK equation of state (de Santis et al., 1974). *K* is the equilibrium constant for the reaction $H_2O + CO_2 = H_2O$-CO_2 complex.

i	***j***	$a_{i,j}$
Non-polar	Non-polar	$[a_i a_j]^{0.5}$
Non-polar	H_2O or CO_2	$[a_i a_j^{(0)}]^{0.5}$
H_2O	CO_2	$[a_i^{(0)} a_j^{(0)}]^{0.5} + 0.5\, R^2 T^{2.5} K$

Table 3: Commonly-used oxygen buffers, expressed in the form $\log (fO_2) = A/T + B + C(P-1)/T$, with *T* in Kelvin and *P* in bars. See also Figure 4(a,b). Buffer equilibria compiled in Frost (1991).

Buffer	**Equilibrium constants**			**Temperature range (°C)**		**Equilibrium reaction**
	A	**B**	**C**	**Min**	**Max**	
αQIF	-29435.7	7.391	0.044	423	~573*	Fe2SiO4 = 2Fe + SiO2 + O_2
βQIF	-29520.8	7.492	0.050	~573*	900	Fe2SiO4 = 2Fe + SiO2 + O_2
IW	-27489.0	6.702	0.055	565	1200	2 FexO = 2x Fe + O_2
WM	-32807.0	13.012	0.083	565	1200	2x/(4x-3) Fe3O4 = 6/(4x-3) FexO + O_2
IM	-28690.6	8.130	0.056	300	565	0.5 Fe3O4 = 1.5 Fe + O_2
CoCoO	-24332.6	7.295	0.052	600	1200	2 CoO = 2 Co + O_2
FMαQ	-26445.3	10.344	0.092	400	~573*	2 Fe3O4 + 3 SiO2 = 3Fe2SiO4 + O_2
FMβQ	-25096.3	8.735	0.110	~573*	1200	2 Fe3O4 + 3 SiO2 = 3Fe2SiO4 + O_2
NiNiO	-24930.0	9.360	0.046	600	1200	2 NiO = 2 Ni + O_2
MH	-25497.5	14.330	0.019	300	573	6 Fe2O3 = 4 Fe3O4 + O_2
MH	-26452.6	15.455	0.019	846	955	6 Fe2O3 = 4 Fe3O4 + O_2
MH	-25700.6	14.558	0.019	955	1373	6 Fe2O3 = 4 Fe3O4 + O_2

* Alpha-beta quartz transition at T [°C] = 573 + 0.025 P [bar].

References

Belonoshko, A. and Saxena, S.K., 1991. A Molecular-Dynamics Study of the Pressure-Volume-Temperature Properties of Supercritical Fluids .2. Co2, Ch4, Co, O2, and H-2. Geochimica Et Cosmochimica Acta, 55(11): 3191-3208.

Blank, J.G., Delaney, J.R. and Desmarais, D.J., 1993. The Concentration and Isotopic Composition of Carbon in Basaltic Glasses from the Juan-De-Fuca Ridge, Pacific-Ocean. Geochimica Et Cosmochimica Acta, 57(4): 875-887.

Bottinga, Y., 1968. Calculation of Fractionation Factors for Carbon and Oxygen Isotopic Exchange in the System Calcite-Carbon Dioxide-Water. Journal of Physical Chemistry, 72: 800.

Bottinga, Y., 1969. Carbon isotope fractionation between graphite, diamond and carbon dioxide. Earth and Planetary Science Letters, 5(5): 301-307.

Brasier, M.D. et al., 2002. Questioning the evidence for Earth's oldest fossils. Nature, 416: 76-81.

Brasier, M.D. et al., 2005. Critical testing of earth's oldest putative fossil assemblage from the similar to 3.5 Ga Apex Chert, Chinaman Creek, western Australia. Precambrian Research, 140(1-2): 55-102.

Carothers, W.W., Adami, L.H. and Rosenbauer, R.J., 1988. Experimental Oxygen Isotope Fractionation between Siderite-Water and Phosphoric-Acid Liberated Co2-Siderite. Geochimica Et Cosmochimica Acta, 52(10): 2445-2450.

Chacko, T., Cole, D.R. and Horita, J., 2001. Equilibrium oxygen, hydrogen and carbon isotope fractionation factors applicable to geologic systems. Stable Isotope Geochemistry, 43: 1-81.

Chacko, T., Mayeda, T.K., Clayton, R.N. and Goldsmith, J.R., 1991. Oxygen and Carbon Isotope Fractionations between Co2 and Calcite. Geochimica Et Cosmochimica Acta, 55(10): 2867-2882.

Chase, M.W., 1998. NIST-JANAF Thermochemical Tables, Fourth edition. Journal of Physical and Chemical Reference Data, Monograph 9.

Chung, H.M., Gormlya, J.R. and Squiresa, R.M., 1988. Origin of gaseous hydrocarbons in subsurface environments: Theoretical considerations of carbon isotope distribution. Chemical Geology, 71(1-3): 97-104.

Clayton, R.N., Goldsmith, J.R., Karel, K.J., Mayeda, T.K. and Newton, R.C., 1975. Limits on Effect of Pressure on Isotopic Fractionation. Geochimica Et Cosmochimica Acta, 39(8): 1197-1201.

Connolly, J.A.D., 1995. Phase-Diagram Methods for Graphitic Rocks and Application to the System C-O-H-Feo-Tio2sio2. Contributions to Mineralogy and Petrology, 119(1): 94-116.

de Santis, R.D., Breedvelde, G.F.J. and J.M., P., 1974. Thermodynamic Properties of Aqueous Gas-Mixtures at Advanced Pressures. Industrial & Engineering Chemistry, Process Design and Development, 13(4): 374-377.

Deines, P., 1980. The Carbon Isotopic Composition of Diamonds - Relationship to Diamond Shape, Color, Occurrence and Vapor Composition. Geochimica Et Cosmochimica Acta, 44(7): 943-961.

Des Marais, D.J. and Moore, J.G., 1984. Carbon and Its Isotopes in Mid-Oceanic Basaltic Glasses. Earth and Planetary Science Letters, 69(1): 43-57.

Dunn, S.R. and Valley, J.W., 1992. Calcite Graphite Isotope Thermometry - a Test for Polymetamorphism in Marble, Tudor Gabbro Aureole, Ontario, Canada. Journal of Metamorphic Geology, 10(4): 487-501.

Flowers, G.C., 1979. Correction of Holloways (1977) Adaptation of the Modified Redlich-Kwong Equation of State for Calculation of the Fugacities of Molecular-Species in Supercritical Fluids of Geologic Interest. Contributions to Mineralogy and Petrology, 69(3): 315-318.

French, B.M., 1971. Stability relations of siderite (FeCO3): thermal decomposition in equilibrium with graphite. American Journal of Science, 271: 37-78.

French, B.M. and Eugster, H.P., 1965. Experimental control of oxygen fugacities by graphite-gas equilibriums. Journal of Geophysical Research, 70: 1529-1539.

French, B.M. and Rosenberg, P.E., 1965. Siderite (FeCO3): thermal decomposition in equilibrium with graphite. Science, 147: 1283-1284.

Frost, B.R., 1979. Mineral Equilibria Involving Mixed-Volatiles in a C-O-H Fluid Phase - Stabilities of Graphite and Siderite. American Journal of Science, 279(9): 1033-1059.

Frost, B.R., 1991. In: D.H. Lindsley (Editor), Oxide Minerals: petrologic and magnetic significance.

Frost, D.J. and Wood, B.J., 1995. Experimental Measurements of the Graphite C-O Equilibrium and Co2 Fugacities at High-Temperature and Pressure. Contributions to Mineralogy and Petrology, 121(3): 303-308.

Gerlach, T.M. and Taylor, B.E., 1990. Carbon Isotope Constraints on Degassing of Carbon-Dioxide from Kilauea Volcano. Geochimica Et Cosmochimica Acta, 54(7): 2051-2058.

Goldsmith, J.R., Graf, D.I., Witters, J. and Northrop, D.A., 1962. Studies in the system CaCO3-MgCO3-FeCO3: 1. Phase relations; 2. A method for major element spectrochemical analysis; 3. Compositions of some ferroan dolomites. Journal of Geology, 70: 659-688.

Golyshev, S.I., Padalko, N.L. and Pechenkin, S.A., 1981. Fractionation of Stable Isotopes of Carbon and Oxygen in Carbonate Systems. Geokhimiya(10): 1427-1441.

Hall, D.L. and Bodnar, R.J., 1990. Methane in Fluid Inclusions from Granulites - a Product of Hydrogen Diffusion. Geochimica Et Cosmochimica Acta, 54(3): 641-651.

Hamann, S.D., Shaw, R.M., Lusk, J. and Batts, B.D., 1984. Isotopic Volume Differences - the Possible Influence of Pressure on the Distribution of Sulfur Isotopes between Sulfide Minerals. Australian Journal of Chemistry, 37(10): 1979-1989.

Hoefs, J., 1975. Ein Beitrag zur Isotopengeochemie das Kohlenstoffs in mamatischen Gesteinen. Fortschrift Mineralogie, 52: 475-478.

Holloway, J.R., 1984. Graphite-Ch4-H2o-Co2 Equilibria at Low-Grade Metamorphic Conditions. Geology, 12(8): 455-458.

Horita, J., 2001. Carbon isotope exchange in the system CO2-CH4 at elevated temperatures. Geochimica Et Cosmochimica Acta, 65(12): 1907-1919.

Huizenga, J.M., 2001. Thermodynamic modelling of C-O-H fluids. Lithos, 55(1-4): 101-114.

Javoy, M. and Pineau, F., 1991. The volatile record of a "popping" rock from the Mid-Atlantic Ridge at 14 degrees N: Chemical and isotopic composition of gas trapped in the vesicles. Earth and Planet. Sci. Lett., 107: 598-611.

Jimenez-Lopez, C. and Romanek, C.S., 2004. Precipitation kinetics and carbon isotope partitioning of inorganic siderite at 25 degrees C and 1 atm. Geochimica Et Cosmochimica Acta, 68(3): 557-571.

Joy, H.W. and Libby, W.F., 1960. Size effects among isotopic molecules. Journal of Chemical Physics, 33(4): 1276.

Kelley, D.S. and Fruh-Green, G.L., 1999. Abiogenic methane in deep-seated mid-ocean ridge environments: Insights from stable isotope analyses. Journal of Geophysical Research-Solid Earth, 104(B5): 10439-10460.

Kerrick, D.M., 1974. Review of Metamorphic Mixed-Volatile (H2o-Co2) Equilibria. American Mineralogist, 59(7-8): 729-762.

Kerrick, D.M. and Jacobs, G.K., 1981. A Modified Redlich-Kwong Equation for H2o, Co2, and H2o-Co2 Mixtures at Elevated Pressures and Temperatures. American Journal of Science, 281(6): 735-767.

Kharlashina, N.N. and Polyakov, V.B., 1992. The Effect of Pressure on the Equilibrium Isotope Fractionation in Minerals - Silicates, Calcite, Rutile. Geokhimiya, 2: 189-200.

Kitchen, N.E. and Valley, J.W., 1995. Carbon-Isotope Thermometry in Marbles of the Adirondack Mountains, New-York. Journal of Metamorphic Geology, 13(5): 577-594.

Koziol, A.M., 2004. Experimental determination of siderite stability and application to Martian Meteorite ALH84001. American Mineralogist, 89(2-3): 294-300.

Marshall, C.P. et al., 2007. Structural characterization of kerogen in 3.4 Ga Archaean cherts from the Pilbara Craton, Western Australia. Precambrian Reasearch, 155: 1-23.

Matsuhisa, Y., Goldsmith, J.R. and Clayton, R.N., 1979. Oxygen Isotopic Fractionation in the System Quartz-Albite-Anorthite-Water. Geochimica Et Cosmochimica Acta, 43(7): 1131-1140.

Mattey, D.P., Carr, R.H., Wright, I.P. and Pillinger, C.T., 1984. Carbon Isotopes in Submarine Basalts. Earth and Planetary Science Letters, 70(2): 196-206.

Matthews, A., Goldsmith, J.R. and Clayton, R.N., 1983a. On the mechanisms and kinetics of oxygen isotope exchange in quartz and feldspars at elevated temperatures and pressures. Geological Society of America Bulletin, 94(3): 396-412.

Matthews, A., Goldsmith, J.R. and Clayton, R.N., 1983b. Oxygen isotope fractionation between zoisite and water. Geochemica et Cosmochimica Acta, 47(3): 645-654.

Matthews, A., Goldsmith, J.R. and Clayton, R.N., 1983c. Oxygen isotope fractionations involving pyroxenes; the calibration of mineral-pair geothermometers. Geochemica et Cosmochimica Acta, 47(3): 631-644.

McCollom, T.M., 2003. Formation of meteorite hydrocarbons from thermal decomposition of siderite (FeCO3). Geochemica et Cosmochimica Acta, 67(2): 311-317.

McCollom, T.M., 2004. Experimental study of potential sources of organic carbon in rocks from the Early Earth, Astrobiology Science Conference. Cambridge, NASA/AIMS, pp. 99.

McKay, D.S. et al., 1996. Search for past life on Mars: possible relic biogenic activity in martian meteorite ALH84001. Science, 273: 924-930.

McSween, H.Y.J., 1997. Evidence for life in a martian meteorite? GSA Today, 7(7): 1-7.

McSween, H.Y.J. and Harvey, R.P., 1998. An evaporation model for formation of carbonates in the ALH84001 martian meteorite. International Geology Review, 40: 774-783.

Mel'nik, Y.P., 1982. Precambrian banded iron-formations, physicochemical conditions of formation. Developments in Precambrian Geology, 5. Elsevier, Amsterdam.

Mojzsis, S.J. et al., 1996. Evidence for life on earth before 3,800 million years ago. Nature, 384(7 November): 55-59.

Mojzsis, S.J. and Harrison, T.M., 2000. Vestiges of a beginning: clues to the emergant biosphere recorded in the oldest known sedimentary rocks. GSA Today, 10(4): 1-6.

Morikiyo, T., 1984. Carbon Isotopic Study on Coexisting Calcite and Graphite in the Ryoke Metamorphic Rocks, Northern Kiso District, Central Japan. Contributions to Mineralogy and Petrology, 87(3): 251-259.

Ohmoto, H. and Kerrick, D., 1977. Devolatilization Equilibria in Graphitic Systems. American Journal of Science, 277(8): 1013-1044.

Pineau, F. and Mathez, E.A., 1990. Carbon Isotopes in Xenoliths from the Hualalai Volcano, Hawaii, and the Generation of Isotopic Variability. Geochimica Et Cosmochimica Acta, 54(1): 217-227.

Polyakov, V.B. and Kharlashina, N.N., 1995a. The Use of Heat-Capacity Data to Calculate Carbon-Isotope Fractionation between Graphite, Diamond, and Carbon-Dioxide - a New Approach. Geochimica Et Cosmochimica Acta, 59(12): 2561-2572.

Polyakov, V.B. and Kharlashina, N.N., 1995b. Direct Calculation of Graphite and Diamond Beta-Factor Values by Use of Heat-Capacity Experimental-Data. Geokhimiya, 8: 1213-1227.

Prausnitz, 1969. Molecular Thermodynamics of Fluid-Phase Equilbria. Prentice-Hall, Englewood Cliffs, N.J., 156 pp.

Price, L.C., 1979. Aqueous Solubility of Methane at Elevated Pressures and Temperatures. American Association of Petroleum Geologists Bulletin, 63(9): 1527-1533.

Redlich, O. and Kwong, J.N.S., 1949. On the Thermodynamics of Solutions. V: An Equation of State. Fugacities of Gaseous Solutions. Chemical Review, 44: 233-244.

Richet and Bottinga, Y., 1977. A review of hydrogen, carbon, nitrogen, oxygen, sulphur, and chlorine stable isotope fractionation among gaseous molecules. Annual Review of Earth and Planetary Science, 5: 65-110.

Rosenberg, P.E., 1967. Subsolidus relations in the system CaCO3-MgCO3-FeCO3 between 350 C and 550 C. American Mineralogist, 52: 787-796.

Rosing, M.T., 1999. ^{13}C-depleted carbon microparticles in >3700-Ma sea-floor sedimentary rocks from west Greenland. Science, 283(29 January): 74-76.

Scheele, N. and Hoefs, J., 1992. Carbon Isotope Fractionation between Calcite, Graphite and Co2 - an Experimental-Study. Contributions to Mineralogy and Petrology, 112(1): 35-45.

Schidlowski, M., 1988. A 3800-million-year isotopic record of life from carbon in sedimentary rocks. Nature, 333(26 May): 313-318.

Schidlowski, M., 1993. The beginnings of life on Earth: evidence from the geological record. In: J.M. Greenberg, C.X. Mendoza-Gomez and V. Pirronello (Editors), The Chemistry of Life's Origins. Kluwer Academic Publishers, Netherlands, pp. 389-414.

Schidlowski, M., 2001. Carbon isotopes as biogeochemical recorders of life over 3.8 Ga of Earth history: evolution of a concept. Precambrian Research, 106(1-2): 117-134.

Schidlowski, M., Appel, P.W.U., Eichmann, R. and Junge, E., 1979. Carbon isotope geochemistry of the 3.7 x 10^9-yr-old Isua sediments, west Greenland: implications for the Archaean carbon and oxygen cycles. Geochimica et Cosmochimica Acta, 43: 189-199.

Schopf, J.W., Kudryavtsev, A.B., Agresti, D.G., Wdowiak, T.J. and Czaja, A.D., 2002. Laser-Raman imagery of Earth's earliest fossils. Nature, 416: 73-76.

Schopf, J.W. and Packer, B.M., 1987. Early Archean (3.3-billion to 3.5-billion-year-old) microfossils from Warrawoona Group, Australia. Science, 237: 70-73.

Sharp, Z.D., Papike, J.J. and Durakiewicz, T., 2003. The effect of thermal decarbonation on stable isotope compositions of carbonates. American Mineralogist, 88(1): 87-92.

Shock, E.L., 1992. Chemical Environments of Submarine Hydrothermal Systems. Origins of Life and Evolution of the Biosphere, 22(1-4): 67-107.

Sugisaki, R. and Mimura, K., 1994. Mantle Hydrocarbons - Abiotic or Biotic. Geochimica Et Cosmochimica Acta, 58(11): 2527-2542.

Swart, P.K., Pillinger, C.T., Milledge, H.J. and Seal, M., 1983. Carbon Isotopic Variation within Individual Diamonds. Nature, 303(5920): 793-795.

Takenouchi, S. and Kennedy, G.C., 1964. The binary system H2O-CO2 at high temperatures and pressures. American Journal of Science, 262: 1055-1074.

Ueno, Y., Yoshioka, H., Maruyama, S. and Isozaki, Y., 2004. Carbon isotopes and petrography of kerogens in similar to 3.5-Ga hydrothermal silica dikes in the North Pole area, Western Australia. Geochimica Et Cosmochimica Acta, 68(3): 573-589.

Valley, J.W. and Oneil, J.R., 1981. C-13-C-12 Exchange between Calcite and Graphite - a Possible Thermometer in Grenville Marbles. Geochimica Et Cosmochimica Acta, 45(3): 411-419.

van Zuilen, M.A., Lepland, A. and Arrhenius, G., 2002. Reassessing the evidence for the earliest traces of life. Nature, 418: 627-630.

van Zuilen, M.A. et al., 2003. Graphite and carbonates in the 3.8 Ga old Isua Supracrustal Belt, southern West Greenland. Precambrian Research, 126(3-4): 331-348.

Wada, H. and Suzuki, K., 1983. Carbon Isotopic Thermometry Calibrated by Dolomite-Calcite Solvus Temperatures. Geochimica Et Cosmochimica Acta, 47(4): 697-706.

Weidner, J.R., 1968. Phase equilibria in a portion of the system Fe-C-O from 250. to 10000 bars and 400 °C to 1200 °C and its petrologic significance, Pennsylvania State University, 162 pp.

Weidner, J.R., 1972. Equilibria in the system Fe-C-O part I: siderite-magnetite-carbon-vapor equilibrium from 500 to 10,000 bars. American Journal of Science, 272: 735-751.

Yui, S., 1966. Decomposition of siderite to magnetite at lower oxygen fugacities: a thermodynamical interpretation and geological implications. Economic Geology, 61: 768-776.

Zhang, C.L. et al., 2001. Temperature-dependent oxygen and carbon isotope fractionations of biogenic siderite. Geochimica Et Cosmochimica Acta, 65(14): 2257-2271.